Received: 27 June 2025 | Accepted: 18 August 2025

DOI: 10.1002/msp2.70015

Malignancy Spectrum

ORIGINAL ARTICLE

Immune infiltration in *TP53* missense mutant contributes to poor prognosis in hepatocellular carcinoma, unlike *CTNNB1* mutations

Durgadevi Veeraiyan[1] | **Vishnu Kurpad**[2] | **Vinayak Munirathnam**[3] | **Chaitra V.**[4] | **Sonal Asthana**[5] | **Akhileshwar Namani**[1] | **Tapas Patra**[1]

[1]Department of Molecular Oncology, Sri Shankara National Centre for Cancer Prevention and Research, Bangalore, India

[2]Department of Surgical Oncology, Sri Shankara Cancer Hospital and Research Centre, Bangalore, India

[3]Department of Medical Oncology, Sri Shankara Cancer Hospital and Research Centre, Bangalore, India

[4]Department of Ono-Pathology, Sri Shankara Cancer Hospital and Research Centre, Bangalore, India

[5]Department of Hepatobiliary and Multiorgan Transplantation Surgery, Aster CMI Hospital, Bangalore, India

Correspondence

Tapas Patra, Department of Molecular Oncology, Sri Shankara National Centre for Cancer Prevention and Research, 1st Cross, Shankara Matt Premises, Shankarapuram, Basavanagudi, Bangalore, Karnataka 560004, India.
Email: tapaspatra@ssnccpr.org and tpatra012@gmail.com

Abstract

Background: Hepatocellular carcinoma (HCC) is one of the deadliest cancer over the world. In this study, we aimed to determine the most critical molecular event in HCC patients with tumor protein p53 (*TP53*) or catenin beta 1 (*CTNNB1*) mutations, and to explore how these two mutations differ in their impact on HCC prognostication.

Methods: We performed an integrated comparative analysis of exome and transcriptome data from The Cancer Genome Atlas (TCGA) for HCC patients. Patient prognosis and correlation with the immune infiltration characteristics were performed. HCC cell line based in vitro experiments were also performed to validate the mechanistic insights.

Results: The 3-year progression-free survival (PFS) analysis of HCC patients with *TP53* mutations indicated a significantly poorer clinical outcome compared to those with *CTNNB1* mutations. Functional annotation of the *TP53* mutant cohort revealed a substantial upregulation of genes associated with immune regulation, while the *CTNNB1* mutant cohort displayed a prominent activation of metabolic pathways. Further comparative analysis and in vitro experiments showed that *TP53* missense mutations activated the signal transducer and activator of transcription 3 (STAT3) signaling pathway, which fostered neutrophil infiltration and enhanced the enrichment of regulatory T (Treg) cells by secreting specific inflammatory molecules in the tumor microenvironment. Notably, treatment with a an STAT3 inhibitor suppressed the expression of these inflammatory molecules, underscoring how an immunosuppressive tumor microenvironment in the *TP53* mutant cohort contributes to a poor prognosis.

Conclusion: Our study provides valuable insights, revealing that HCC patients with *TP53* missense mutations exhibit a distinct immune profile associated with poorer clinical outcome compared to those with *CTNNB1* mutations.

KEYWORDS

hepatocellular carcinoma, progression-free survival, gene expression, p53, β-catenin, neutrophil, T regulatory cell, chemokine, signal transduction, The Cancer Genome Atlas

This is an open access article under the terms of the Creative Commons Attribution License, which permits use, distribution and reproduction in any medium, provided the original work is properly cited.
© 2025 The Author(s). *Malignancy Spectrum* published by John Wiley & Sons Australia, Ltd on behalf of Higher Education Press.

INTRODUCTION

Hepatocellular carcinoma (HCC) is the sixth most common malignancy and the third most common cause of cancer-related death worldwide. Currently, the 5-year survival rate of HCC patients is less than 20%, while the 5-year recurrence and metastasis rates are even higher than 88% [1]. Major risk factor of HCC includes viral infections, nonalcoholic fatty liver disease, and alcohol consumption. Late diagnosis, limited treatment options, and complex etiology contribute to poor prognosis and high mortality rates in HCC patients. Genetic alterations in HCC often include somatic mutations in the telomerase reverse transcriptase (*TERT*), tumor protein p53 (*TP53*), catenin beta 1 (*CTNNB1*), axis inhibition protein 1 (*AXIN1*), and the AT-rich interacting domain-containing protein 1A *(ARID1A*) genes. Among these genetic alterations, *TP53* and *CTNNB1* are the most potent oncogenic driver mutations of HCC, with occurrence rate around 30% [2]. An oncogenic driver mutation is a genetic alteration that actively contributes to the initiation and progression of cancer. These mutations confer a growth or survival advantage to cells, promoting uncontrolled proliferation and tumor development. They are fundamental to the cancerous transformation of normal cells. In contrast, passenger mutations are incidental genetic changes that accumulate during cancer development but do not play a direct role in driving the disease. Understanding the oncogenic driver mutations enables oncologists to tailor treatments that specifically target cancer-related pathways, potentially resulting in more effective therapies and improved patient outcomes. The common *TP53* mutation confers activities in the signaling pathways for tumor development and progression, in addition to abrogating the tumor suppressing capacity. The mutated *CTNNB1* plays an oncogenic role [3, 4]. However, it remains entirely unclear which molecular event has the most significant impact in HCC patients harboring *TP53* or *CTNNB1* mutations, and what differences exist between these two mutations in regulating the prognosis of HCC. Nevertheless, molecular prognosis is the less explored area in HCC. In this study, we aimed to address the questions through an integrated database analysis.

METHODS

Patient data collection

All the HCC patient-related data included in the current study were handled according to the previous publication [5]. Briefly, the somatic mutational information from exome sequencing data, transcriptomic information from RNA sequencing (RNA-seq) data, and other relevant clinical information were downloaded from The Cancer Genome Atlas Liver Hepatocellular Carcinoma (TCGA-LIHC) project. The immunotherapeutic treatment data of HCC patients with mutational status were obtained from The Hepatocellular Carcinoma—Memorial Sloan Kettering Integrated Mutation Profiling of Actionable Cancer Targets (MSK-IMPACT) project through cBioportal dataset.

Survival analysis

We analyzed 3-year progression-free survival (PFS) by Cox proportional hazards model and generated the Kaplan–Meier curves using XLSTAT software.

Differential gene expression with functional enrichment

According to the somatic mutations of *TP53* and *CTNNB1* in TCGA-LIHC, data were split into mutant and wild-type groups. The differential gene expression analysis was performed and adopted the following criterion: $\log_2$ (fold change) > 2.0 was set as the threshold for upregulated genes. Based on the upregulated genes, we performed functional enrichment analysis through Kyoto Encyclopedia of Genes and Genomes (KEGG) pathway using DAVID 6.8 database [6]. The protein expression levels of the *TP53*-mutated group were also examined using the reverse-phase protein array (RPPA) dataset from TCGA-LIHC.

Tumor microenvironment assessment

Based on the differentially expressed genes between mutated groups, the immune cell infiltration and correlation analysis with particular gene expression were performed using the TIMER 2.0 database using similar TCGA-LHIC datasets [7].

Cell culture

Cell culture was performed following previous publication [8]. Briefly, six HCC cell lines were purchased from the American Type Culture Collection (ATCC) and maintained in our laboratory. All the cell lines were cultured in Dulbecco's modified Eagle's medium (Gibco) supplemented with 10% fetal bovine serum, 1% Penstrep (Hyclone), and maintained at 37°C in a humidified 5% CO_2 incubator. Cell lines were treated with the signal transducer and activator of transcription 3 (STAT3) inhibitor Stattic at 2.5 µmol/L for 24 h. The dose and incubation time we chose were from previous study, in which treatment with 2.5 µmol/L Stattic for 24 h caused only inhibition of

STAT3 phosphorylation, without affecting the cell proliferation and phosphorylation of extracellular signal-regulated kinase (ERK) [9].

Quantitative reverse-transcription polymerase chain reaction(qRT-PCR)

qRT-PCR was performed following previous publication [10]. Briefly, total RNA was extracted from HCC cell lines using TRIzol. cDNAs were synthesized through reverse transcription with cDNA Synthesis Kit (Thermo) and then analyzed by real-time PCR using the SYBR Green detection system (Applied Biosystem) on a QuantStudio instrument (Applied Biosystem). The RT-PCR amplification was conducted for 40 cycles. Glyceraldehyde 3-phosphate dehydrogenase gene was set as control to normalize the 11 target genes. The relative gene expression was analyzed using the $2^{-\Delta\Delta CT}$ formula ($\Delta\Delta CT = \Delta CT$ of the sample – ΔCT of the control).

Western blot analysis

Western blot analysis was performed following previous publication [11]. Briefly, cultured cells were lysed in RIPA buffer containing 1% PMSF to extract total protein. Protein concentration was determined using the BCA protein assay kit (Thermo). Equal amounts of protein from each group were separated by 10% sodium dodecyl sulphate-polyacrylamide gel electrophoresis (SDS-PAGE) and transferred to a nitrocellulose membrane (Bio-Rad). After blocking with 5% BSA for 1 h, the membrane was incubated overnight at 4°C with primary antibodies targeting the proteins of interest, followed by incubation with HRP-conjugated secondary antibodies at room temperature for 1 h. Bands were visualized using ECL reagent (Thermo). The Phospho-STAT3 (T705) and internal control β-actin antibodies were purchased from Cell Signaling Technology.

Statistical analysis

The differential expression of complements in TIMER was explored using the Wilcoxon test. Survival was evaluated using the Kaplan-Meier plotter combined with the log-rank test. The correlations between variables were examined using Pearson correlation. When analyzing data from three or more groups, analysis of variance was performed, and a *t*-test was employed when comparing data between two groups. p-values < 0.05 were considered statistically significant.

RESULTS AND DISCUSSION

Comparative impact of *TP53* and *CTNNB1* mutations on the survival of HCC patients

TP53 and *CTNNB1*, the most frequently mutated genes, are considered the dominant cancer drivers for HCC development, with variable frequencies depending on the etiology [12]. In this study, cBioportal was used to investigate the mutational landscape of *TP53* and *CTNNB1* genes in HCC from TCGA pan-cancer dataset. The overall analysis was conducted in a cohort of 362 HCC patients, in which 110 patients (31%) carried *TP53* mutations and 95 patients (27%) carried *CTNNB1* mutations. Almost 6% (21) of the HCC patients carried mutations in both genes (Figure 1a). About 82% of *CTNNB1* mutations were located in beta-transducin repeat containing protein (β-TrCP)-recognition site where phosphorylated β-catenin is degraded by ubiquitination. Almost all *CTNNB1* mutations (92%) were missense type which prevent ubiquitination of the protein and stabilize for its oncogenic functions. About 66% of *TP53* mutations were missense and 89% of the mutations were located at the DNA binding domain, indicating that p53 loses its transcriptional activation and tumor suppressor functions (Figure 1b). Figure 1c shows the distribution of disease stages among cohorts carrying mutations in the *CTNNB1* and *TP53* genes. The data indicate that there is no strong correlation between disease stage and the presence of either *CTNNB1* or *TP53* mutations. Through deep introspection, it was observed that *CTNNB1* mutations were slightly higher in stage I, IIIA, and IIIC, whereas *TP53* mutations were slightly higher in stage II and IV (Figure 1c). One earlier study suggested that *TP53* mutations are detected with high frequency in advanced HCC patients [13]. Across the literature survey, while some patterns exist, the correlation is not strong or consistent enough across global datasets to definitively associate *TP53* or *CTNNB1* mutations with viral or nonviral HCC etiology. Between mutations of these two driver genes, which one has greater impact on the prognostication of HCC? The low survival rate of HCC patients is primarily driven by late-stage diagnosis, where the median survival is 1–3 years and the 5-year survival rate is less than 20%. For this reason, we considered to analyze 3-year PFS in HCC patients who did not have either *TP53* or *CTNNB1* mutations, who had only *TP53* but not *CTNNB1* mutations, and who had only *CTNNB1* but not *TP53* mutations. From the Kaplan-Meier plot, we observed that patients with *TP53* mutations had significantly worse PFS than those who did not have any *TP53* or *CTNNB1* mutations, or had only *CTNNB1* but not *TP53* mutations. However, we did not find any difference in PFS between patients carrying the *CTNNB1* mutations and those who did not have either *TP53* or *CTNNB1* mutations

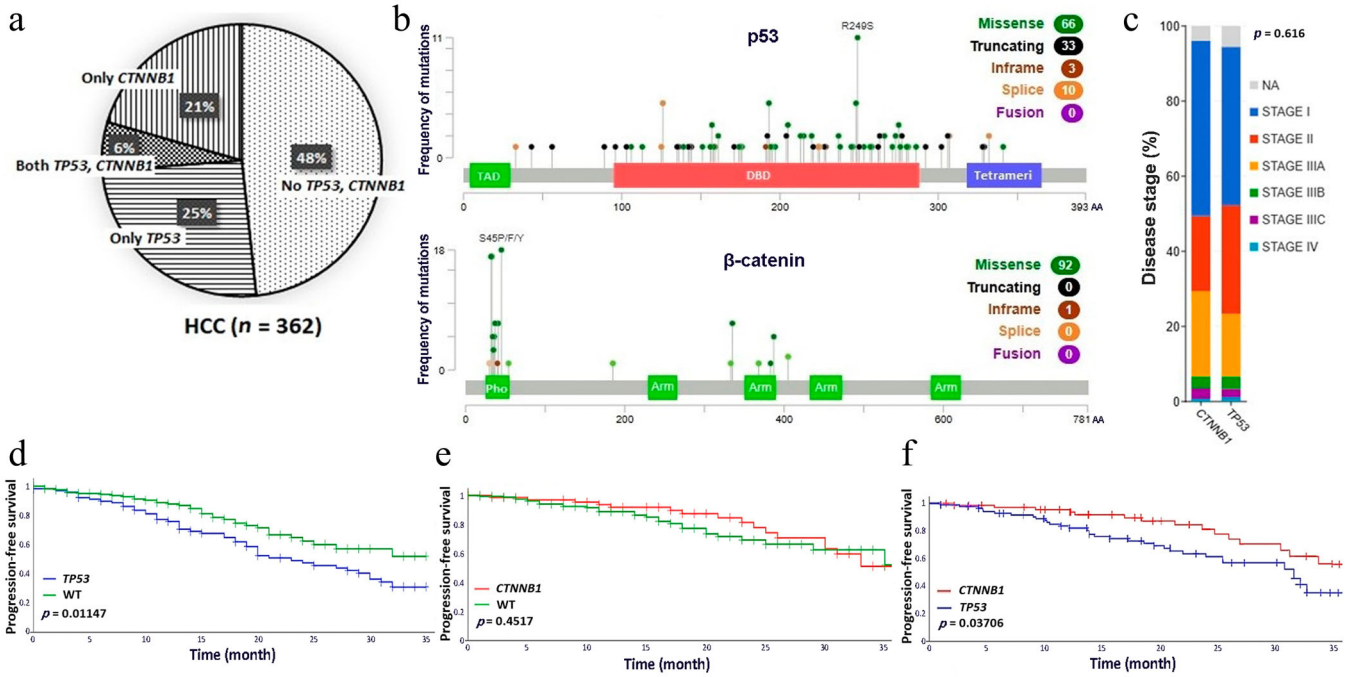

FIGURE 1 The prognostic value of *TP53* and *CTNNB1* genetic alterations in hepatocellular carcinoma (HCC). (a) Pie chart showing the percentage frequencies of *TP53* and *CTNNB1* mutations harboured within HCC cohort. (b) Lollipop plots representing the positions of mutations on the functional domains of p53 and β-catenin proteins. The types of mutations are also mentioned in the diagram. (c) The stacked bar charts showing the percentage of disease stage in the cohorts carrying the mutations of *CTNNB1* and *TP53* genes. (d–f) Kaplan–Meier plots revealing significant differences in progression-free survival among HCC patients harboring only *TP53* mutations, only *CTNNB1* mutations, or neither of these two gene mutations. *p*-values are shown inside the figures and $p < 0.05$ is considered statistically significant.

(Figure 1d–f). Thus, the 3-year PFS analysis of HCC patients with *TP53* mutations indicates a poor clinical outcome, irrespective of disease stage.

Functional enrichment of upregulated genes from *TP53 and CTNNB1* mutational cohorts

To determine the reason for the disparate PFS between HCC cohorts with *TP53* and *CTNNB1* mutations, an integrated differential gene expression analysis was performed. We observed that 160 genes were considerably upregulated in the patient cohort that carrying only *CTNNB1* mutations while 154 genes were significantly elevated in *TP53* mutational cohort, and 34 upregulated genes were reciprocally present in both cohorts. For purposeful understanding of differential gene expression of both cohorts, we separately performed gene set enrichment analysis (GSEA). Functional annotation of the *TP53* mutant cohort showed that significant number of upregulated genes precisely involved in inflammatory response pathway, neutrophil chemotaxis, and transforming growth factor-β (TGF-β) receptor-mediated signaling (Figure 2a). On the other hand, the *CTNNB1* mutant cohort significantly represented upregulation of several metabolic pathways including xenobiotics, small molecules, steroids, or heterocycles (Figure 2b). Hence, the dysregulation of certain immune response pathways was associated with worse PFS in HCC patients with *TP53* mutations.

Correlation of neutrophil infiltration and enriched pathways in HCC patients carrying *TP53* mutations

Based on the GSEA, we extended our analysis to investigate immune cell infiltration in the tumor microenvironment of HCC patients. This approach allowed for a deeper understanding of the immune landscape in HCC, providing insights into the relationship between specific genetic alterations, immune cell profiles, and clinical outcomes in this cancer type. We observed that the *TP53* mutant cohort had higher levels of neutrophil infiltration compared to the *CTNNB1* mutant cohort (Figure 3a,b). Certain members of CXC chemokine family, such as chemokine (C-X-C motif) ligand 1 (CXCL1), CXCL5, and CXCL6, play an essential role in the inflammatory process by directing neutrophils to the site of infection or injury [14–16]. Vanin-2 (VNN2) is an enzyme linked to oxidative stress and inflammatory pathways that can influence neutrophil trafficking [17]. Interleukin-17C (IL-17C) is an epithelial cytokine

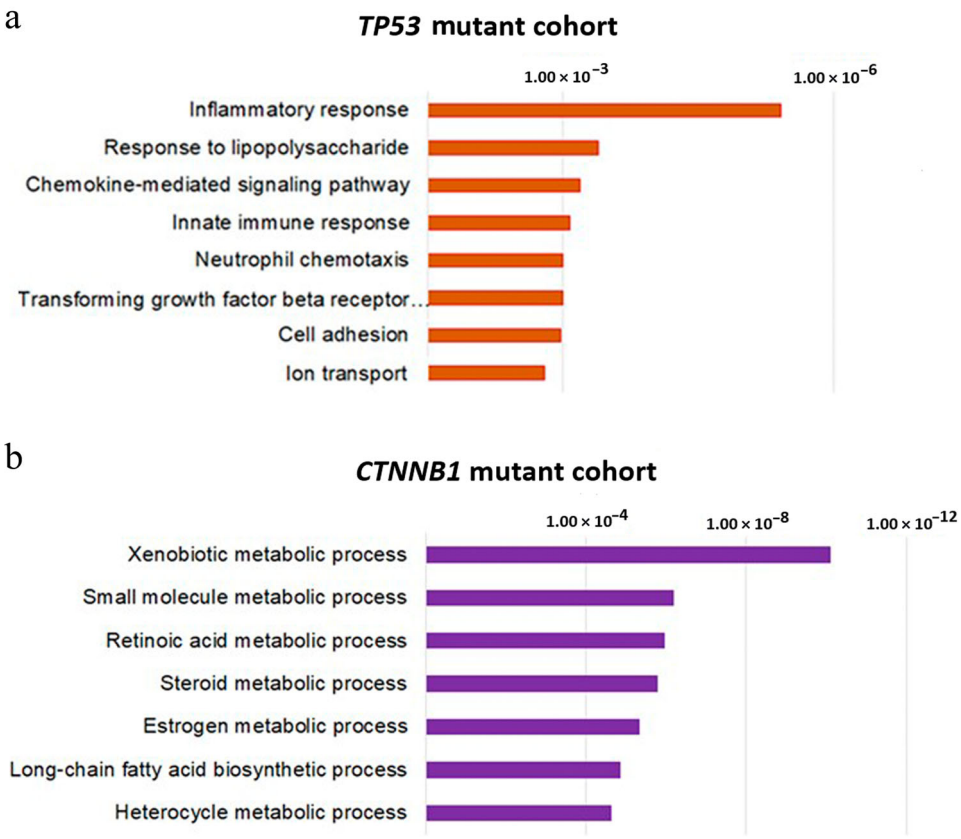

FIGURE 2 Gene enrichment patterns in *TP53* and *CTNNB1* mutant cohorts. (a, b) Horizontal bar plot presenting gene set functional enrichment analyses of the significantly upregulated genes in the *TP53* (a) and *CTNNB1* (b) mutational cohorts.

closely associated with neutrophil recruitment [18]. There was an increase in the expression of *CXCL1*, *CXCL5*, *CXCL6*, *VNN2*, and *IL-17C* in our cohort of samples with mutations in the *TP53* gene. The upregulation of these inflammatory molecules was strongly correlated with higher levels of neutrophil infiltration into the tumor tissue (Figure 3c–g).

Neutrophil infiltration connects with regulatory T cell enrichment in *TP53* mutational cohort

In the context of cancer, TGF-β signaling has a dual role. Initially, it can act as a tumor suppressor by inhibiting cell proliferation and promoting apoptosis. However, as tumors progress, TGF-β often becomes a promoter of immune suppression and tumor progression [19]. Our study also showed that specifically, *TGFB2* and TGF-β receptor 2 (*TGFBR2*) were significantly upregulated in the *TP53* mutant cohort (Figure 4a,b). In a TGF-β-mediated environment, the presence of high levels of neutrophils can lead to the secretion of inflammatory molecules like S100A8, arginase 1 (ARG1), CCL17, and CCL22 by neutrophils, which can promote the differentiation and expansion of regulatory T (Treg) cells [20, 21]. We noticed that inflammatory molecules S100A8, ARG1, CCL17, and CCL22 were upregulated and correlated with high levels of Treg infiltration in *TP53* mutant cohort (Figure 4c–f). Additionally, our study also revealed that the *TP53* mutant cohort exhibited a more pronounced enrichment of Treg cells within the tumor microenvironment compared with the *CTNNB1* mutant (Figure 4g,h). An elevated level of immunosuppressive cytokines within the tumor microenvironment has been shown to drive neutrophil polarization towards the N2 phenotype, which is characterized by protumorigenic and immunosuppressive functions [22]. These N2-polarized neutrophils further contribute to tumor immune evasion by promoting the differentiation and expansion of Treg cells through the secretion of specific chemokines and signalling molecules [23–26]. Therefore, the current study indicates the dominance of certain inflammatory molecules, due to a particular genetic alteration, is responsible for increased neutrophil infiltration, which subsequently leads to accumulation of Treg cells at the tumor site.

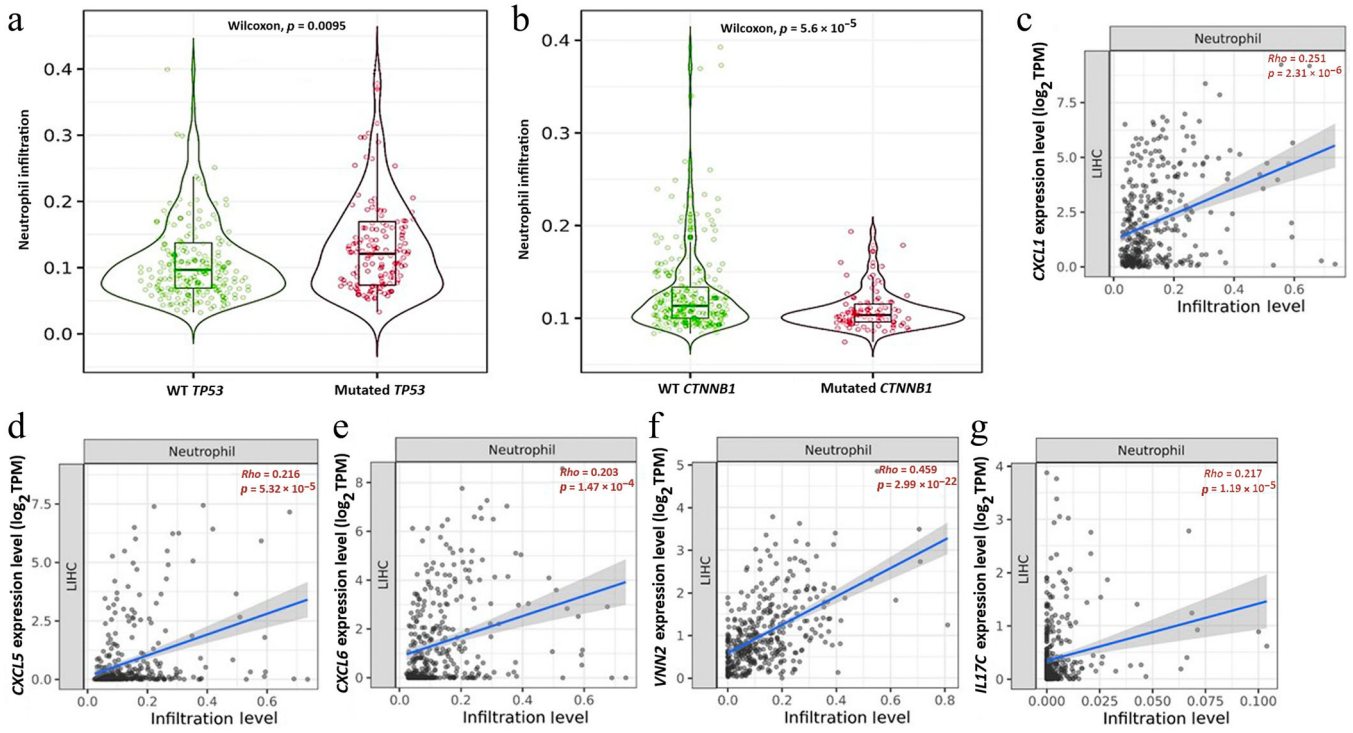

FIGURE 3 Impact of neutrophil infiltration on enriched pathways in *TP53*-driven HCC. (a, b) Violin plots comparing the difference in neutrophil infiltration between mutant and wild type in the *TP53* and *CTNNB1* mutational cohorts. (c–g) Plots showing the correlations of gene expression of *CXCL1*, *CXCL5*, *CXCL6*, *VNN2*, and *IL-17C* with neutrophil infiltration in *TP53* mutant cohort. *p*-values are shown inside the figures and $p < 0.05$ is considered statistically significant.

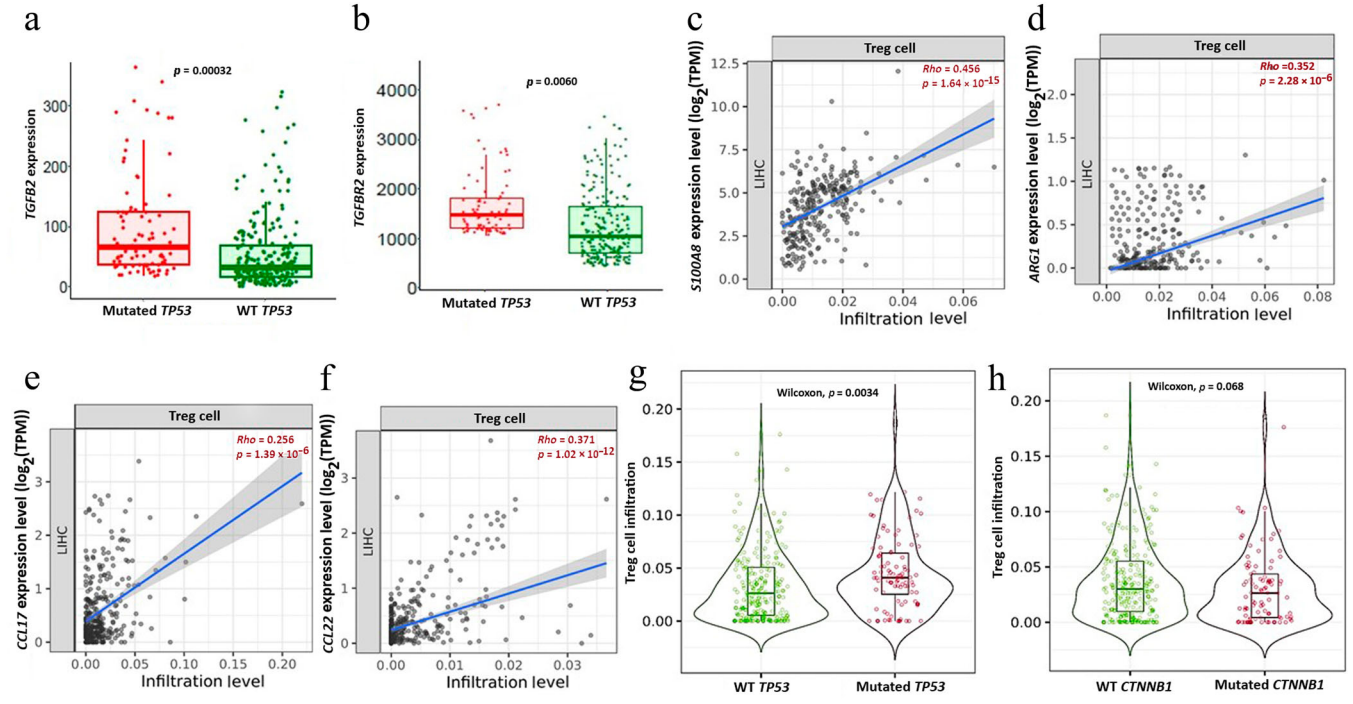

FIGURE 4 Correlation of neutrophil infiltration with Treg cell enrichment in *TP53* mutant cohort. (a, b) Box plots comparing the expression levels of *TGFB2* and *TGFBR2* between mutant and wild type in the *TP53* mutational cohorts. (c–f) Plots showing the correlations of gene expression of *S100A8*, *ARG1*, *CCL17*, and *CCL22* with Treg cell enrichment in *TP53* mutant cohort. (g, h) Violin plots comparing the differences in Treg cell infiltration betwen mutant and wild type in the *TP53* and *CTNNB1* mutational cohorts. *p*-values are shown inside the figures and $p < 0.05$ is considered statistically significant.

Prognostication of immune infiltration associates with *TP53* mutations in HCC

In support of our observations, Zhou et al. showed that overexpression of CXCL5 mediates neutrophil infiltration and indicates poor prognosis for HCC [27]. Next, we examined whether infiltration of these particular immune cells does have any prognostic value. The results revealed that high levels of neutrophil infiltration in tumor microenvironment were associated with significantly worse 3-year disease-free survival (DFS) compared to low levels of neutrophil infiltration (Figure 5a). We also found that high Treg cell enrichment in HCC tissue led to significantly poorer DFS compared with low Treg cell enrichment (Figure 5b). In another mutant cohort, high expression levels of the metabolic genes, uridine diphosphate glucuronosyl transferase 1A1 (*UGT1A1*), cytochrome P450 family 1 subfamily A member 2 (*CYP1A2*), and alcohol dehydrogenase 4 (*ADH4*), were significantly associated with *CTNNB1* mutations. However, it was found that there was no significant difference in 3-year DFS between high and low expression of these metabolic genes (Figure 5c–e). Thus, an immunosuppressive tumor microenvironment led to an unfavourable prognostic value in the *TP53* mutant cohort.

Mechanistic relationship between immune infiltration and *TP53* mutations

The question now arises: how the *TP53* mutations affect the induction of specific immuno-modulatory molecules that promote neutrophil infiltration in the HCC microenvironment. Several studies have already reported that particularly *TP53* missense mutations at DNA binding domain of the protein accumulate misfolded p53 in the tumor cell and alter the cellular behaviors [28–30]. Recently, it has been published that missense mutation-derived misfolded p53 protein interacts with heat shock protein 90 to form a complex which prevents degradation of phospho-STAT3 and activates the downstream signaling pathway [31]. From the cBioportal RPPA datasets, a marked increase in STAT3 Tyr705 phosphorylation was observed in the *TP53* mutant cohort compared to *CTNNB1* mutant cohort (Figure 6a). To explore further, we conducted an *in vitro* investigation using cell line models. We selected six HCC cell lines with different mutational features: PLC/PRF5 having *TP53* missense mutation (R249S) and *CTNNB1*-wild type; HLF having *TP53* missense mutation (G244A) and *CTNNB1*-wild type; HLE having *TP53* missense mutation (G244A) and *CTNNB1*-wild

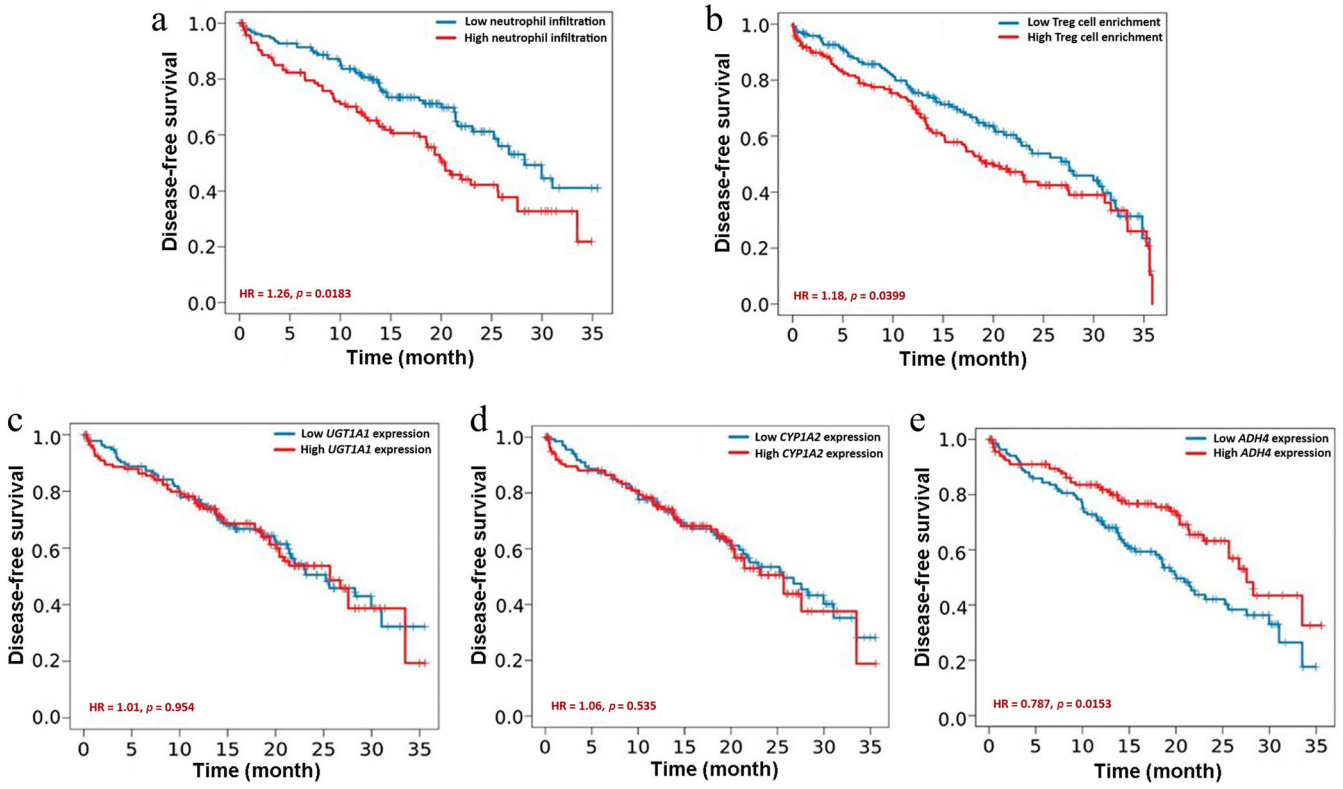

FIGURE 5 Survival analysis of immune infiltration associated with *TP53* mutations and gene enrichment in *CTNNB1* mutant cohort. (a, b) Kaplan–Meier plots displaying the differential DFS based on the high or low levels of neutrophil infiltration and Treg cell enrichment in *TP53* mutational cohorts. (c–e) Kaplan–Meier plots exhibiting the differential DFS based on the gene expression of *UGT1A1*, *CYP1A2*, and *ADH4* in *CTNNB1* mutational cohorts. *p*-values are shown inside the figures and $p < 0.05$ is considered statistically significant.

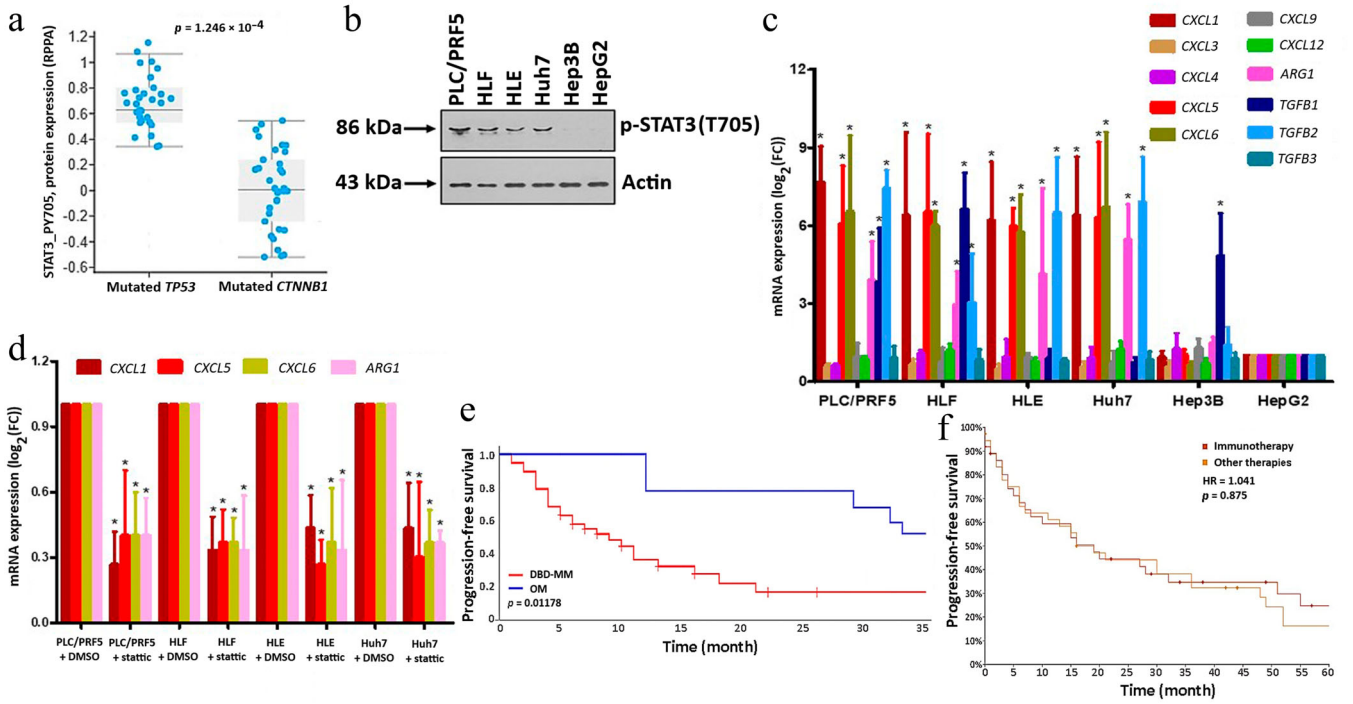

FIGURE 6 Immune infiltration dynamics and the interaction with *TP53* missense mutations. (a) Box plot representing the levels of phosphorylated STAT3 protein in *TP53* and *CTNNB1* mutational HCC cohorts. (b) Western blot showing the levels of phosphorylated STAT3 protein in six different HCC cell lines. Actin are used for internal control. (c) Bar graph indicating the transcript levels of different inflammatory molecules in six different HCC cell lines. (d) Bar graph indicating the transcript levels of different inflammatory molecules with or without treatment of STAT3 inhibitor Stattic (2.5 μmol/lL) in HCC cell lines carrying *TP53* missense mutations for 24 h. (e) Kaplan–Meier plots exhibiting the differential PFS based on *TP53* missense mutations in DNA-binding domain (abbreviated as DBD-MM) and other *TP53* mutations (abbreviated as as OM). (f) Kaplan–Meier plots showing the differential PFS based on *TP53* mutational HCC cohort that received either immune checkpoint inhibitor or other therapies. *p*-values are shown inside the figures and "*", $p < 0.05$ is considered statistically significant.

type; Huh7 having *TP53* missense mutation (Y220C) and *CTNNB1*-wild type; Hep3B having *TP53* truncated deletion mutation and *CTNNB1*-wild type; HepG2 having *TP53*-wild type and *CTNNB1* exon3 deletion. Western blot analysis showed that phosphorylated STAT3 was detected in *TP53* missense mutant cell lines, but not detected in *TP53* truncated mutant or wild-type lines. (Figure 6b). STAT3 signaling pathway regulates some specific inflammatory molecules like CXCL1, CXCL5, CXCL6, ARG1, and TGF-β [32–35]. Next, qRT-PCR experiment was performed to analyze the transcript levels of immuno-modulatory molecules in these HCC cell lines. it was observed that the transcript levels of *CXCL1*, *CXCL5*, *CXCL6*, and *ARG1* were elevated in the *TP53* missense mutant cell lines compared to *TP53* truncated mutant or wild type cell lines. The other CXCL genes like *CXCL3*, *CXCL4*, and *CXCL9* remained unchanged in all cell lines. The expression levels of *TGFB1* and *TGFB2* were not consistent, whereas *TGFB3* was not expressed enough in all cell lines (Figure 6c). To verify further, we treated those cell lines with STAT3 inhibitor Stattic. The transcript levels of upregulated molecules, *CXCL1*, *CXCL5*, *CXCL6*, and *ARG1*, were suppressed after Static treatment (Figure 6d). In addition, the PFS of HCC patients with *TP53* mutations was analyzed, respectively. Comparative analysis showed that the PFS of patients with *TP53* missense mutations was worse than that of patients with other types of *TP53* mutations (Figure 6e).

Our study found that HCC patients with *TP53* mutations exhibited increased neutrophil infiltration. However, we were unable to determine whether this neutrophil infiltration was linked to the systemic neutrophil-lymphocyte ratio (NLR), as our database did not include the relevant clinical data. It is well established that NLR is a clinical parameter that is significantly associated with prognostication in HCC patients [36], and NLR has been shown to correlate with T lymphocyte infiltration only in gastric cancer patients [37]. To address this gap, a future study will explore the relationship between neutrophil infiltration and NLR in HCC patients. Consequently, our current findings offer the potential to develop a systemic biomarker for identifying HCC patients with poor survival outcomes.

Combination therapy consisting of an anti-programmed death ligand-1 (PD-L1) inhibitor plus either an anti-cytotoxic T-lymphocyte-associated

antigen 4 (CTLA-4) immune checkpoint inhibitor (ICI) or anti-vascular endothelial growth factor (VEGF) therapy continues to be the standard first-line treatment for advanced HCC. Some studies suggest that patients with nonviral HCC may exhibit a less favourable response to ICIs compared to those with virus-associated HCC. To date, no predictive biomarkers for ICI treatment in HCC patients have been prospectively validated or approved. The question now is, what would happen if these patients underwent ICI treatment? To answer this question, we analyzed the PFS of HCC patients harbouring *TP53* mutations, using their treatment records from the MSK datasets available in cBioPortal. Treatment with ICI did not yield a better response compared to other therapies received by the HCC patients with *TP53* mutations (Figure 6f). Therefore, novel therapeutic strategies, such as incorporating STAT inhibitors into standard regimens like ICI therapy, are urgently needed, especially for HCC patients carrying *TP53* missense mutations.

Our current work has several limitations. The analysis relies on data from various databases, each of which has inherent constraints that may influence the findings. These limitations include potential biases in patient selection, variability in therapeutic interventions, and the quality of the data. Additionally, this study primarily involves *in silico* analysis and lacks experimental or clinical validation. Therefore, further research is necessary to confirm these results in HCC patients in future studies.

A similar study was conducted by Yang et al., who performed a comprehensive analysis of *TP53* mutations in HCC and constructed a prognostic risk model based on the gene expression profiles [38]. The study also mentioned that HCC patients with *TP53* mutations have a bad prognosis with immunosuppressive phenotypic regulation. Our study, however, offers distinct and complementary mechanistic insights. Specifically, we directly compared the survival impact of *TP53* versus *CTNNB1* mutations, the two most common driver mutations in HCC patients, demonstrating that *TP53* mutations, particularly missense mutations, are more strongly associated with poor PFS. Furthermore, we explored the immune microenvironment of *TP53* mutated tumors, and revealed that enhanced neutrophil infiltration and the accumulation of Treg cells, mediated via the activation of STAT3-dependent immunosuppressive signaling, as key mechanisms underlying the worse clinical outcomes. *In vitro* validation using HCC cell lines, coupled with the response analysis of STAT3 inhibition further underscores the translational importance of our findings. Thus, our study extends beyond prognostic modeling to uncover the mechanistic pathways that link *TP53* mutations to immune evasion and therapy resistance, providing a compelling rationale for novel therapeutic strategies, such as combining STAT3 inhibitors with ICI therapy in *TP53* mutant HCC patients. Notably, prior studies in other cancer types have also reported a link between *TP53* mutations and elevated neutrophil infiltration, lending further support to our findings. For example, *TP53* mutations have been shown to be associated with increased neutrophil recruitment in pancreatic cancer [39], glioblastoma [40], and lung adenocarcinoma [41]. The growing body of evidence provides us with greater confidence to pursue future investigations aimed at elucidating the systemic impact of *TP53* mutations on tumor–immune interactions in HCC.

CONCLUSION

Based on the most frequent somatic driver mutations, our study demonstrates that *TP53* mutations are linked to a unique immune signature and confer a worse prognosis in HCC patients compared to *CTNNB1* mutations. Particularly, missense mutations in *TP53* gene are likely driven by the activation of the STAT3 pathway, which promotes the infiltration of neutrophils and the enrichment of Treg cells in the tumor immune microenvironment. These findings highlight the importance of performing genetic profiling in HCC patients after diagnosis to guide treatment stratification and facilitate the development of personalized therapeutic approaches.

AUTHOR CONTRIBUTIONS

Durgadevi Veeraiyan: Methodology. **Vishnu Kurpad**: Writing and formal analysis. **Vinayak Munirathnam**: Formal analysis and data curation. **Chaitra V.**: Methodology and data curation. **Sonal Asthana**: Review and editing. **Akhileshwar Namani**: Methodology. **Tapas Patra**: Conceptualization, review and editing, investigation, methodology, formal analysis, data curation, and supervision.

ACKNOWLEDGEMENTS

We thank the Sri Shankara Cancer Foundation. We received research funds from Megh Steel Pvt Ltd., Bangalore.

CONFLICT OF INTEREST STATEMENT

The authors declare no conflicts of interest.

DATA AVAILABILITY STATEMENT

The datasets used and/or analyzed during the current study are available from the corresponding author on reasonable request. Data are derived from public domain resources.

ETHICS STATEMENT

The authors have nothing to report.

REFERENCES

1. Rumgay H, Arnold M, Ferlay J, et al. Global burden of primary liver cancer in 2020 and predictions to 2040. *J Hepatol*. 2022; 77(6):1598-1606.
2. Dhanasekaran R, Nault JC, Roberts LR, Zucman-Rossi J. Genomic medicine and implications for hepatocellular carcinoma prevention and therapy. *Gastroenterology*. 2019;156(2): 492-509.
3. Hassin O, Oren M. Drugging p53 in cancer: one protein, many targets. *Nat Rev Drug Discovery*. 2023;22(2):127-144.
4. Kim S, Jeong S. Mutation hotspots in the β-catenin gene: lessons from the human cancer genome databases. *Mol Cells*. 2019;42(1):8-16.
5. Namani A, Veeraiyan D, Patra T. A comparative analysis indicates SLC7A11 expression regulate the prognostic value of *KEAP1-NFE2L2-CUL3* mutations in human uterine corpus endometrial carcinoma. *Free Radic Biol Med*. 2024;222:223-228.
6. Sherman BT, Hao M, Qiu J, et al. DAVID: a web server for functional enrichment analysis and functional annotation of gene lists (2021 update). *Nucleic Acids Res*. 2022;50(W1): W216-W221.
7. Li T, Fu J, Zeng Z, et al. TIMER2.0 for analysis of tumor-infiltrating immune cells. *Nucleic Acids Res*. 2020;48(W1): W509-W514.
8. Patra T, Meyer K, Ray RB, Kanda T, Ray R. Akt inhibitor augments anti-proliferative efficacy of a dual mTORC1/2 inhibitor by FOXO3a activation in p53-mutated hepatocarcinoma cells. *Cell Death Dis*. 2021;12(11):1073.
9. Lin L, Jou D, Wang Y, et al. STAT3 as a potential therapeutic target in $ALDH^+$ and $CD44^+/CD24^+$ stem cell-like pancreatic cancer cells. *Int J Oncol*. 2016;49(6):2265-2274.
10. Patra T, Sasaki R, Meyer K, Ray RB, Ray R. Transforming growth factor β acts as a regulatory molecule for lipogenic pathways among hepatitis C virus genotype-specific infections. *J Virol*. 2019;93(18):e00811-19.
11. Murmu N, Ghosh P, Namani A, Patra T. Glyoxylate supplementation ameliorates colitis associated colon cancer progression. *J Cell Physiol*. 2024;239(11):e31394.
12. Schulze K, Imbeaud S, Letouzé E, et al. Exome sequencing of hepatocellular carcinomas identifies new mutational signatures and potential therapeutic targets. *Nat Genet*. 2015;47(5): 505-511.
13. Lombardo D, Saitta C, Giosa D, et al. Frequency of somatic mutations in *TERT* promoter, *TP53* and *CTNNB1* genes in patients with hepatocellular carcinoma from Southern Italy. *Oncol Lett*. 2020;19(3):2368-2374.
14. Koch AE, Kunkel SL, Harlow LA, et al. Epithelial neutrophil activating peptide-78: a novel chemotactic cytokine for neutrophils in arthritis. *J Clin Invest*. 1994;94(3):1012-1018.
15. Jovic S, Linge HM, Shikhagaie MM, et al. The neutrophil-recruiting chemokine GCP-2/CXCL6 is expressed in cystic fibrosis airways and retains its functional properties after binding to extracellular DNA. *Mucosal Immunol*. 2016;9(1):112-123.
16. Yadav SK, Stojkov D, Feigelson SW, et al. Chemokine-triggered microtubule polymerization promotes neutrophil chemotaxis and invasion but not transendothelial migration. *J Leukoc Biol*. 2019;105(4):755-766.
17. Nitto T, Onodera K. The linkage between coenzyme A metabolism and inflammation: roles of pantetheinase. *J Pharmacol Sci*. 2013;123(1):1-8.
18. Jungnickel C, Schmidt LH, Bittigkoffer L, et al. IL-17C mediates the recruitment of tumor-associated neutrophils and lung tumor growth. *Oncogene*. 2017;36(29):4182-4190.
19. Yang L, Moses HL. Transforming growth factor β: tumor suppressor or promoter? Are host immune cells the answer? *Cancer Res*. 2008;68(22):9107-9111.
20. Sippel TR, White J, Nag K, et al. Neutrophil degranulation and immunosuppression in patients with GBM: restoration of cellular immune function by targeting arginase I. *Clin Cancer Res*. 2011;17(22):6992-7002.
21. Maruyama T, Kono K, Izawa S, et al. CCL17 and CCL22 chemokines within tumor microenvironment are related to infiltration of regulatory T cells in esophageal squamous cell carcinoma. *Dis Esophagus*. 2010;23(5):422-429.
22. Antuamwine BB, Bosnjakovic R, Hofmann-Vega F, et al. N1 versus N2 and PMN-MDSC: a critical appraisal of current concepts on tumor-associated neutrophils and new directions for human oncology. *Immunol Rev*. 2023;314(1):250-279.
23. Zhou SL, Zhou ZJ, Hu ZQ, et al. Tumor-associated neutrophils recruit macrophages and T-regulatory cells to promote progression of hepatocellular carcinoma and resistance to sorafenib. *Gastroenterology*. 2016;150(7):1646-1658.
24. Zou JM, Qin J, Li YC, et al. IL-35 induces N2 phenotype of neutrophils to promote tumor growth. *Oncotarget*. 2017;8(20): 33501-33514.
25. Rodriguez PC, Quiceno DG, Ochoa AC. L-arginine availability regulates T-lymphocyte cell-cycle progression. *Blood*. 2007; 109(4):1568-1573.
26. Zhang F, Xia Y, Su J, et al. Neutrophil diversity and function in health and disease. *Signal Transduct Target Ther*. 2024;9(1): 343.
27. Zhou SL, Dai Z, Zhou ZJ, et al. Overexpression of CXCL5 mediates neutrophil infiltration and indicates poor prognosis for hepatocellular carcinoma. *Hepatology*. 2012;56(6):2242-2254.
28. Végran F, Rebucci M, Chevrier S, Cadouot M, Boidot R, Lizard-Nacol S. Only missense mutations affecting the DNA binding domain of p53 influence outcomes in patients with breast carcinoma. *PLoS One*. 2013;8(1):e55103.
29. Zhu J, Sammons MA, Donahue G, et al. Gain-of-function p53 mutants co-opt chromatin pathways to drive cancer growth. *Nature*. 2015;525(7568):206-211.
30. López I, P. Oliveira L, Tucci P, Álvarez-Valín F, A. Coudry R, Marín M. Different mutation profiles associated to P53 accumulation in colorectal cancer. *Gene*. 2012;499(1):81-87.
31. Schulz-Heddergott R, Stark N, Edmunds SJ, et al. Therapeutic ablation of gain-of-function mutant p53 in colorectal cancer inhibits Stat3-mediated tumor growth and invasion. *Cancer Cell*. 2018;34(2):298-314.
32. Traber KE, Hilliard KL, Allen E, et al. Induction of STAT3-dependent CXCL5 expression and neutrophil recruitment by oncostatin-M during pneumonia. *Am J Respir Cell Mol Biol*. 2015;53(4):479-488.
33. Vasquez-Dunddel D, Pan F, Zeng Q, et al. STAT3 regulates arginase-I in myeloid-derived suppressor cells from cancer patients. *J Clin Invest*. 2013;123(4):1580-1589.
34. Lu H, Ai J, Zheng Y, et al. IGFBP2/ITGA5 promotes gefitinib resistance via activating STAT3/CXCL1 axis in non-small cell lung cancer. *Cell Death Dis*. 2024;15(6):447.
35. Song M, He J, Pan QZ, et al. Cancer-associated fibroblast-mediated cellular crosstalk supports hepatocellular carcinoma progression. *Hepatology*. 2021;73(5):1717-1735.
36. Wang C, Wang M, Zhang X, et al. The neutrophil-to-lymphocyte ratio is a predictive factor for the survival of patients with hepatocellular carcinoma undergoing transarterial chemoembolization. *Ann Transl Med*. 2020;8(8):541.
37. He Q, Huangfu L, Fan B, et al. T-cells infiltration mediates the association between neutrophil/lymphocyte ratio and survival in gastric cancer. *Cancer Med*. 2023;12(15):15893-15902.
38. Yang Y, Qu Y, Li Z, Tan Z, Lei Y, Bai S. Identification of novel characteristics in TP53-mutant hepatocellular carcinoma using bioinformatics. *Front Genet*. 2022;13:874805.
39. Siolas D, Vucic E, Kurz E, Hajdu C, Bar-Sagi D. Gain-of-function $p53^{R172H}$ mutation drives accumulation of neutrophils

in pancreatic tumors, promoting resistance to immunotherapy. *Cell Rep*. 2021;36(8):109578.
40. Ham SW, Jeon HY, Jin X, et al. *TP53* gain-of-function mutation promotes inflammation in glioblastoma. *Cell Death Differ*. 2019; 26(3):409-425.
41. Ye Y, Luo Y, Sun Y, et al. Single-cell transcriptomic profiling reveals KRAS/TP53-driven neutrophil reprogramming in LUAD: a multi-gene prognostic model and therapeutic targeting of RHOV. *Oncol Res*. 2025;33(6): 1383-1404.

How to cite this article: Veeraiyan D, Kurpad V, Munirathnam V, et al. Immune infiltration in *TP53* missense mutant contributes to poor prognosis in hepatocellular carcinoma, unlike *CTNNB1* mutations. *Malig Spect*. 2025;2(3):117-127. doi:10.1002/msp2.70015